Available online at http://scik.org

Commun. Math. Biol. Neurosci. 2024, 2024:77

https://doi.org/10.28919/cmbn/8667

ISSN: 2052-2541

THE IMPACTS OF PREY HARVESTING ACTIVITY ON THE STABILITY OF AN EXTREME FISHERY SYSTEM WITH PREY CARRION BIOMASS RESOURCES

WAN NATASHA WAN HUSSIN[1,*], HAMIZAH MOHD SAFUAN[1], TAU KEONG ANG[2]

[1]Center of Research for Computational Mathematics, Department of Mathematics and Statistics, Faculty of Applied Sciences and Technology, Universiti Tun Hussein Onn Malaysia, 84600 Pagoh, Johor, Malaysia

[2]Department of Mathematical Sciences, Faculty of Science, Universiti Teknologi Malaysia, 81310 Skudai, Johor Bahru, Malaysia

Abstract: This research analyzes the interaction of prey and carnivorous apex facultative scavengers in the existence of prey carrion biomass. Prey consists of vertebrate marine animals as the main food preferences for carnivorous apex facultative scavengers, which comprise fish, reptiles and marine mammals, whose carrion is also hunted and eaten. Apex facultative scavengers or formidable predators are superior in scavenging, where they can search and consume carrion more efficiently than other scavengers. The fishery system is assumed to be in an extreme condition where the temperature in marine life habitat is high due to climate change. There, the survival of apex facultative scavengers in the marine system only depends on their predation and scavenging interactions with prey and prey carrion biomass, respectively. Moreover, prey carrion biomass formation only relies on the predation interaction of prey and apex facultative scavengers due to its limited source. Apex facultative scavengers can be extinct without the existence of prey. Both prey and apex facultative scavenger populations are harvested due to their commercial values. However, the dynamical behaviors of the fishery model have been analyzed by considering prey harvesting as a bifurcation parameter due to their importance in determining the stability of an extreme fishery system since prey are the main

*Corresponding author

E-mail address: wan.natasha123@gmail.com

Received May 29, 2024

source of apex facultative scavengers growth and prey carrion biomass formation. It is found that the underharvesting of prey leads to the appearance of periodic oscillations around unstable coexistence equilibrium through Hopf bifurcation. The intermediate level of prey harvesting guarantees the coexistence of all interacting populations, and their high level of harvesting implies the appearance of the bistability phenomenon and saddle-node bifurcation of the steady-states in the fishery system. Lastly, the overharvesting of prey makes the extreme fishery system collapse.

Keywords: prey-prey carrion biomass-apex facultative scavenger; prey harvesting; predation; scavenging; local bifurcations; bistability.

2020 AMS Subject Classification: 34A34, 34C23, 34C60, 92B05, 92D25, 92D40.

1. INTRODUCTION

In a fishery ecosystem, along with prey and predator populations, there also exists a type of animal that feeds on the dead animal's leftovers, which is called a scavenger. The major food source for aquatic scavengers is fishery discards. Examples of aquatic scavengers that feed on carrion (the flesh of dead animals) are mackerel, Atlantic cod, sea bass, remora, spinous spider crab, cuttlefish, shark and conger eel [1]. Shark is an example of a carnivorous apex facultative scavenger that hunts and consumes both live prey and carrion of dead marine animals. Instead of vertebrate marine animals, sharks also consume marine invertebrates like mollusks and crustaceans as their alternative foods. A massive aquatic animal like a shark has a large pectoral fin that prefers to cruise through the water and has been considered a top facultative scavenger [2]. However, sharks have the possibility to compete with their apex predators or competitors like orcas (killer whales) in hunting their same limited food sources [3]. According to Carey et al. [4], sharks are ectotherm fish with low metabolic rates who can go weeks without eating because they prefer the energy-dense parts of carcasses (dead bodies of marine animals). However, sharks in the tropical ocean as well as small sharks have high metabolic rates and are actively searching for their live prey and carrion to survive.

Scavenger research is significant because these organisms assist in cleaning up the environment and controlling disease. Scavengers can consume the carcasses of infected animals without affecting their health [5, 6]. As stated by Motivarash Yagnesh et al. [7], sharks regulate prey populations by removing weak and sick animals, thus maintaining diversity in prey species. Unfortunately, it was estimated that the global amount of marine carrion which is the food source for marine scavengers that come from fisheries discards was 18.8 million tonnes in 1989 and is

currently declining to less than 10 million tonnes annually [8, 9]. The execution of the Landing Obligation (LO), which gradually eliminates discards by minimizing needless catches as much as possible and by slowly ensuring that catches are landed, may destroy the scavenger population [1, 10]. Furthermore, due to animal deaths from natural aging and rapid ingestion by scavengers, there are less naturally occurring marine carrion formations, such as the carrion of seals, dolphins, sea lions, whales and fish.

According to Cheung et al. [11], extreme temperature events have occurred in all ocean basins over the last two decades, harming marine biodiversity, ecosystem functions and services. Using an integrated climate-biodiversity-fisheries-economic impact model, they estimated that when an annual high temperature extreme occurs in an exclusive economic zone, 77% of exploited fish and invertebrates will lose biomass, while maximum catch potential will fall by 6%, adding to the decadal-scale mean impacts of climate change. The net negative impacts of high temperature extremes on fish stocks are expected to result in losses in fisheries revenues and livelihoods in the majority of maritime countries, causing jolts to fishery's social-ecological systems, especially in climate-vulnerable regions. However, in this research, we consider the temperature of the water in the fishery ecosystem which is in the tropical ocean is higher than usual (not too hot) due to climate change. According to Nero et al. [12], the temperature of water in the sea usually decreases with depth below the mixed layer (thermocline) and it has a major impact on the decomposition rate of dead sea turtles where the volume of their internal gases produced to float to the surface of the sea are decreased (Charles' Law) and thus resulting to the nonlinearly decrease in their decomposition rate. The gases like methane, ammonia, hydrogen sulfide and carbon dioxide are produced by aerobic and anaerobic bacteria in the tissues and digestive tract of dead organisms during their decomposition [13].

As opposed to that, the warm and humid environment conditions can accelerate the decomposition rates of carcasses or carrion [14]. Besides, the flora and fauna in the sea may influence the rate of decomposition of marine carrion. The flora or plants like seaweed, algae, seagrass and microscopic algae (phytoplankton) absorb carbon dioxide and release oxygen during their photosynthesis. The oxygen gas is needed for decomposers like bacteria, fungi, marine worm and echinoderm for their respiration and survival in doing the decomposition activity. The ubiquitous existence of marine fauna like scavengers and decomposers in the sea may accelerate the decomposition rate of marine carrion. Moreover, the strong currents in the ocean can cause carcasses to move over long distances and they can probably be scraped along things such as tree

limbs, rocks, the bottom of the body of water and others. These situations will put pressure on the apex facultative scavenger population to hunt their food since marine carrion easily decomposes, and they may confront their apex predators in hunting the same food sources (prey). The prey population can be threatened if the harvesting activity is not controlled, and it can have an adverse effect on the stability of the fishery system.

Realizing the importance of carrion for scavengers, O'Bryan, Holden and Watson [15] have proposed two mathematical models to describe the scavenging interactions between apex obligate scavengers, mesoscavengers and carrion biomass in the first model and considered apex facultative scavengers to replace apex obligate scavengers in the second model. Distinct from facultative scavengers, obligate scavengers are fully dependent on carrion for life. Besides, Mellard et al. [16] have analyzed the effects of scavenging activities by facultative scavengers and primary predators on predation in a four-dimensional food web model. Based on the research of Jana and Panja [17], they discovered that in the presence of extra food for the scavenger species, the disorderly dynamics can be regulated by the quadratic harvesting of predator and scavenger species. Hussin et al. [6] found that scavenging activities by scavengers have a detrimental effect on the prey−predator−scavenger fishery system with scavenger harvesting if they are not properly controlled. Additionally, Zawka and Melese [18] studied the dynamics and ideal harvesting practices of a prey−predator system in the presence of scavengers, which reduced pollution in the environment by eating the carcasses of sick predator and prey.

Previous research studied the effect of carrion source marine animal harvesting on the density of carrion in the fishery systems, but not many studied in terms of bifurcation analysis. Ecologically, carrion is an important food source for scavengers, and research related to scavengers is needed to ensure balanced interaction between these species, which then leads to a balanced fishery ecosystem. Past studies [1, 5, 6, 15−21] have inspired us to investigate the dynamics of the fishery model with prey carrion biomass density and with the existence of carrion source marine animals (prey) and apex facultative scavenger harvesting. We investigate the impacts of prey harvesting on the stability of an extreme fishery system via bifurcation analysis due to the significance of prey population density in the fishery system, which acts as a main food source for carnivorous apex facultative scavengers. We think that the model will lead to more complex dynamics in fishery models' behaviors, which is important for maintaining and conserving the fishery ecosystem.

2. THE MATHEMATICAL MODEL

The mathematical formulation of the current research fishery model is based on previous research by [5, 15, 16]. Differing from previous research, this present work considers the harvesting impacts of prey in an extreme fishery system with prey carrion biomass density. Our approach mainly focuses on bifurcation analysis. The dimensional form of the fishery model is formulated as

$$\frac{dR}{dT} = r_1 R\left(1 - \frac{R}{K_1}\right) - \alpha_1 RS - q_1 E_1 R, \tag{1a}$$

$$\frac{dC}{dT} = \theta\alpha_1 RS - d_1 C - \alpha_2 CS, \tag{1b}$$

$$\frac{dS}{dT} = \phi\alpha_1\beta_1 RS - d_2 S + \alpha_2\beta_2 CS - q_2 E_2 S, \tag{1c}$$

where R, C and S are prey, prey carrion biomass and carnivorous apex facultative scavenger, respectively. Variable T refers to time. Prey grows logistically with the intrinsic growth rate r_1 and carrying capacity K_1. Parameters α_1 and α_2 are attack rates of prey and prey carrion by the apex facultative scavenger, respectively. The conversion rates of prey and prey carrion to apex facultative scavenger density are represented by parameters β_1 and β_2, respectively. The proportion of dead prey that the apex facultative scavenger rapidly eats is represented by the parameter $\phi \in (0,1)$, while the proportion of dead prey that the apex facultative scavenger instantly transforms into carrion is represented by $\theta = 1-\phi$. The rate of prey carrion losses due to other scavenger species and decomposition and the natural mortality rate of apex facultative scavenger are denoted by parameters d_1 and d_2, respectively. The catchability coefficients of the prey and apex facultative scavenger are represented by parameters q_1 and q_2, respectively. Parameters E_1 and E_2 refer to the effort harvesting rates of prey and apex facultative scavenger, respectively. Every parameter is positive, and each variable is not negative.

Kane et al. [22] revealed that carrion production depends on predation, disease and scavenging. In the extreme fishery system (1), we assume the sources of prey carrion are only contributed by the predation interaction between prey and apex facultative scavengers, and both predation and scavenging activities have control over the density of prey carrion. In the absence of prey, apex facultative scavengers can extirpate. In an extreme fishery system (1), we omitted the sources of carrion from the natural deaths of vertebrate marine prey and apex facultative scavengers and

sources of foods other than vertebrate marine prey for apex facultative scavengers due to the limitations of those sources because of the rapid consumption of other scavenger and predator species and the rapid decomposition by decomposers like bacteria, fungi, marine worms and echinoderms due to environment conditions in the marine life habitat that supported decomposition process. Natural mortality refers to the elimination of aquatic animals other than harvesting, such as through natural senescence, disease, competition, cannibalism and pollution.

The factors that may influence the decomposition activity of the marine carrion are water depth, the temperature of the water, water current, the surrounding ecosystem and the existence of flora (marine plants) and fauna (decomposers and scavengers) that support the decomposition process. Because carrion is unpredictable and ephemeral, unlike living prey, scavenging depends more on the potential to move efficiently over greater distances than predation. Instead of the locomotion ability of scavengers, the good sensory detection of carrion through smell ensures faster reach to the carrion.

2.1. Dimensionless fishery model

To make the fishery model easier to analyze, the fishery system (1) is non-dimensionalized, which minimizes the number of parameters in the model. The dimensionless fishery system is given by

$$\frac{dx}{dt} = x(1-x) - xz - \rho x\,, \tag{2a}$$

$$\frac{dy}{dt} = \eta xz - \sigma y - \epsilon yz\,, \tag{2b}$$

$$\frac{dz}{dt} = \omega xz - \kappa z + yz - \delta z\,, \tag{2c}$$

where its non-dimensional variables are

$$x = \frac{R}{K_1}\,, y = \frac{\alpha_2\beta_2 C}{r_1}, z = \frac{\alpha_1 S}{r_1}\,, t = r_1 T,$$

and dimensionless parameters are

$$\rho = \frac{q_1 E_1}{r_1}\,, \eta = \frac{\alpha_2\beta_2\theta K_1}{r_1}, \sigma = \frac{d_1}{r_1}\,, \epsilon = \frac{\alpha_2}{\alpha_1}\,, \omega = \frac{\phi\alpha_1\beta_1 K_1}{r_1}\,, \kappa = \frac{d_2}{r_1}\,, \delta = \frac{q_2 E_2}{r_1}.$$

The dimensionless system (2) is on the set

$$\zeta = \{(x,y,z) \in \mathbb{R}^3 | x \geq 0, y \geq 0, z \geq 0\}. \tag{3}$$

3. THE PRESENCE AND STABILITY OF EQUILIBRIUM

The fishery system (2) equilibria are derived, and their local and global stability is examined in this section. Prey harvesting (ρ) is a bifurcation parameter, and the threshold requirements for the existence of transcritical and saddle-node bifurcations about the equilibrium points or steady-states are studied.

3.1. Existence of steady-states from the fishery model (2)

i. The extinction equilibrium point $P_1 = (0,0,0)$ exists without any parametric restrictions.

ii. The prey-free equilibrium $P_2 = \left(0, \kappa + \delta, -\frac{\sigma}{\epsilon}\right)$ is not biologically meaningful due to the strictly negative value of the equilibrium number of apex facultative scavengers. This steady-state is not considered throughout the analysis of the fishery system (2).

iii. The equilibrium with only the presence of prey, $P_3 = (1-\rho,0,0)$ is feasible if $1-\rho > 0$.

iv. The coexistence steady-state $P_4 = (1-\rho-\hat{z}, \kappa+\delta-\omega\,[1-\rho-\hat{z}],\ \hat{z})$, where $\hat{z}$ is positive root(s) by solving the quadratic polynomial equation of

$$(\eta + \epsilon\omega)\hat{z}^2 + [\sigma\omega + \epsilon(\kappa+\delta) - (\eta+\epsilon\omega)(1-\rho)]\hat{z} + \sigma[\kappa+\delta-\omega(1-\rho)] = 0. \quad (4)$$

The coexistence steady-state P_4 exists or is feasible under the conditions

$$\left[(1-\rho)(\eta+\epsilon\omega) - [\sigma\omega + \epsilon(\kappa+\delta)]\right]^2 \geq 4\sigma(\eta+\epsilon\omega)[\kappa+\delta-\omega(1-\rho)], \quad (5a)$$

$$\sigma\omega + \epsilon(\kappa+\delta) < (1-\rho)(\eta+\epsilon\omega), \quad (5b)$$

$$0 < 1-\rho-\hat{z} < \frac{\kappa+\delta}{\omega}. \quad (5c)$$

3.2. Analysis of the local stability in the steady-states

We investigate the local stability requirements for feasible steady-states of the fishery system (2) based on the linearization method and the Routh-Hurwitz criterion [23−28]. Local stability of the equilibrium points indicates the solutions of the differential equations of the system (2) tend to converge to the equilibrium points under the initial number of interacting populations close to the equilibrium points. Therefore, by considering the Jacobian matrix

$$J(x,y,z) = \begin{pmatrix} 1-\rho-z-2x & 0 & -x \\ \eta z & -\sigma-\epsilon z & \eta x - \epsilon y \\ \omega z & z & \omega x + y - \kappa - \delta \end{pmatrix}, \quad (6)$$

the local stability of the equilibrium points of the fishery system (2) can be investigated.

3.2.1. Stability of $P_1 = (0,0,0)$

The eigenvalues found from the Jacobian matrix (6) derived at equilibrium point P_1 are $\lambda_1 = 1-\rho$, $\lambda_2 = -\sigma$ and $\lambda_3 = -(\kappa+\delta)$. Hence, the extinction equilibrium P_1 is a stable node if $1-\rho < 0$, while it is an unstable saddle point if $1-\rho > 0$. If equilibrium P_1 is a stable node, therefore an equilibrium P_3 is unfeasible due to the unsatisfaction of the condition $1-\rho > 0$, whereas if equilibrium P_1 is an unstable saddle point, hence equilibrium P_3 is feasible because the condition $1-\rho > 0$ is holding. Moreover, if equilibrium P_1 is an unstable saddle point, coexistence equilibrium P_4 can exist as long as the conditions (5a)–(5c) are satisfied, whereas if equilibrium P_1 is a stable node where $1-\rho < 0$, the coexistence equilibrium P_4 does not exist.

Based on this research, the neutral saddle (NS) of equilibrium P_1 describes the nature of its eigenvalues which is the sum of the two eigenvalues is zero and the other eigenvalue is a negative real number. The neutral saddle point is not a bifurcation point, since it is a hyperbolic saddle [29]. Neutral saddle points occur when

$$\rho = 1 - (\kappa + \delta), \tag{7}$$

and

$$\rho = 1 - \sigma, \tag{8}$$

when we treat prey harvesting, ρ as a bifurcation parameter. At steady-state P_1, the necessary criteria for the transcritical bifurcation (TB) to happen when ρ differs is

$$\rho = 1. \tag{9}$$

3.2.2. Stability of $P_3 = (1-\rho,0,0)$

By considering the Jacobian matrix (6) about the steady-state P_3, the eigenvalues obtained are $\lambda_1 = -(1-\rho)$, $\lambda_2 = -\sigma$ and $\lambda_3 = \omega(1-\rho) - (\kappa+\delta)$. Consider the feasibility condition $1-\rho > 0$ for equilibrium P_3 is satisfied. Hence, steady-state P_3 is a stable node if the condition $\kappa+\delta > \omega(1-\rho)$ is satisfied, while it is an unstable saddle point if the condition $\kappa + \delta < \omega(1-\rho)$ is satisfied.

If equilibrium P_3 is a stable node, then equilibrium P_1 is an unstable saddle due to the condition $1-\rho < 0$ not holding, whereas if equilibrium P_3 is an unstable saddle, then equilibrium P_1 also can be the unstable saddle. Besides, if equilibrium P_3 is a stable node, the coexistence equilibrium P_4 may exist as long as conditions in (5a) –(5c) are satisfied. In the condition of equilibrium P_3 is an unstable saddle, it can cause the feasibility of coexistence equilibrium P_4 if criteria in (5b) and (5c) are satisfied.

Regarding this study, neutral saddles of equilibrium P_3 happen when

$$\rho = \sigma + 1, \tag{10}$$

$$\rho = 1 - \left(\frac{\kappa + \delta}{\omega - 1}\right), \tag{11}$$

and

$$\rho = 1 - \left(\frac{\sigma + \kappa + \delta}{\omega}\right), \tag{12}$$

when we treat ρ as a bifurcation parameter. On the other hand, the threshold conditions for the existence of transcritical bifurcation when ρ varies are $\rho = 1$, which is same as a condition in (9) and

$$\rho = \frac{\omega - (\kappa + \delta)}{\omega}. \tag{13}$$

3.2.3. Stability of $P_4 = (1-\rho-\hat{z},\ \kappa+\delta-\omega[1-\rho-\hat{z}],\ \hat{z})$

Based on the Jacobian matrix of system (2) in (6), the Jacobian matrix about the coexistence equilibrium P_4 is given as

$$J_{P_4} = \begin{pmatrix} -(1-\rho-\hat{z}) & 0 & -(1-\rho-\hat{z}) \\ \eta\hat{z} & -(\sigma+\epsilon\hat{z}) & \eta(1-\rho-\hat{z}) - \epsilon[\kappa+\delta-\omega(1-\rho-\hat{z})] \\ \omega\hat{z} & \hat{z} & 0 \end{pmatrix}. \tag{14}$$

Theorem 1. *If all feasibility conditions of the coexistence steady-state P_4 in (5a)−(5c) are satisfied, then the coexistence equilibrium P_4 exists and is locally stable if the conditions*

$$\eta\hat{z} < \sigma + \hat{z}(\epsilon + \omega), \tag{15a}$$

$$\sigma\omega + \epsilon(\kappa + \delta) > (1 - \rho - 2\hat{z})(\eta + \epsilon\omega), \tag{15b}$$

$$\begin{aligned}[1-\rho-\hat{z}] \times [(\sigma + \hat{z}[\epsilon+\omega])(1-\rho-\hat{z}+\sigma+\epsilon\hat{z})] + \epsilon\hat{z}(\sigma+\epsilon\hat{z}) \\ \times [\kappa+\delta-\omega(1-\rho-\hat{z})] > \hat{z}(1-\rho-\hat{z})[(\sigma+\epsilon\hat{z})(\eta+\omega)+\eta\hat{z}],\end{aligned} \tag{15c}$$

are satisfied.

Proof. The coexistence steady-state P_4 characteristic equation is expressed as

$$A_1\lambda^3 + A_2\lambda^2 + A_3\lambda + A_4 = 0, \tag{16}$$

where,

$$A_1 = 1, \tag{17a}$$

$$A_2 = (1-\rho-\hat{z}) + (\sigma+\epsilon\hat{z}), \tag{17b}$$

$$A_3 = (1-\rho-\hat{z})[\sigma+\hat{z}(\epsilon+\omega)-\eta\hat{z}] + \epsilon\hat{z}[\kappa+\delta-\omega(1-\rho-\hat{z})], \tag{17c}$$

$$A_4 = \hat{z}(1-\rho-\hat{z})[\sigma\omega+\epsilon(\kappa+\delta)-(1-\rho-2\hat{z})(\eta+\epsilon\omega)]. \tag{17d}$$

From (17a), A_1 is always positive. If all feasibility conditions of coexistence steady-state P_4 in (5a)–(5c) and conditions in equations (15a) and (15b) are satisfied, therefore A_2, A_3 and A_4 in (17b)–(17d) are all positive. Next, consider the derivation of equation $A_2A_3 - A_1A_4 > 0$ below:

$$[1-\rho-\hat{z}+\sigma+\epsilon\hat{z}] \times \left[(1-\rho-\hat{z})[\sigma+\hat{z}(\epsilon+\omega)-\eta\hat{z}] + \epsilon\hat{z}[\kappa+\delta-\omega(1-\rho-\hat{z})]\right] -$$

$$\hat{z}(1-\rho-\hat{z}) \times [\sigma\omega+\epsilon(\kappa+\delta)-(1-\rho-2\hat{z})(\eta+\epsilon\omega)] > 0.$$

The above equation is equivalent to

$$[1-\rho-\hat{z}+\sigma+\epsilon\hat{z}] \times \left[(1-\rho-\hat{z})[\sigma+\hat{z}(\epsilon+\omega)-\eta\hat{z}] + \epsilon\hat{z}[\kappa+\delta-\omega(1-\rho-\hat{z})]\right] -$$

$$\hat{z}(1-\rho-\hat{z}) \times [\eta\hat{z}+\omega(\sigma+\epsilon\hat{z})+\epsilon(\kappa+\delta-\omega[1-\rho-\hat{z}])-\eta(1-\rho-\hat{z})] > 0.$$

By expanding, factorizing and simplifying the latest equation above, we obtain

$$[1-\rho-\hat{z}] \times [(1-\rho-\hat{z}+\sigma+\epsilon\hat{z})[\sigma+\hat{z}(\epsilon+\omega)-\eta\hat{z}] - \hat{z}(\eta\hat{z}+\omega[\sigma+\epsilon\hat{z}]) + \eta\hat{z}(1-\rho-\hat{z})] + \epsilon\hat{z}(\sigma+\epsilon\hat{z}) \times [\kappa+\delta-\omega(1-\rho-\hat{z})] > 0.$$

Continue to expand, simplify and factorize the like terms, we arrived to

$$[1-\rho-\hat{z}] \times [(\sigma+\hat{z}[\epsilon+\omega])(1-\rho-\hat{z}+\sigma+\epsilon\hat{z}) - \hat{z}([\sigma+\epsilon\hat{z}][\eta+\omega]+\eta\hat{z})] + \epsilon\hat{z}(\sigma+\epsilon\hat{z}) \times [\kappa+\delta-\omega(1-\rho-\hat{z})] > 0,$$

and by rewriting it, lastly, we get

$$[1-\rho-\hat{z}] \times [(\sigma+\hat{z}[\epsilon+\omega])(1-\rho-\hat{z}+\sigma+\epsilon\hat{z})] + \epsilon\hat{z}(\sigma+\epsilon\hat{z}) \times [\kappa+\delta-\omega(1-\rho-\hat{z})] - \hat{z}(1-\rho-\hat{z})[(\sigma+\epsilon\hat{z})(\eta+\omega)+\eta\hat{z}] > 0. \tag{18}$$

Again, if all existence conditions of the coexistence steady-state P_4 and condition in (15c) are satisfied, then the latest equation of $A_2A_3 - A_1A_4$ in (18) is positive. Thus, based on the Routh Hurwitz criterion, it ensures the local stability of the coexistence steady-state P_4. □

If coexistence equilibrium P_4 is stable which is all its feasibility conditions in (5a)–(5c) are satisfied and conditions in (15a)–(15c) are satisfied, then P_1 is an unstable saddle point, whereas if steady-state P_4 is unstable, therefore equilibrium point P_1 also can be an unstable saddle point.

Besides, if the coexistence steady-state P_4 is stable, therefore equilibrium point P_3 is a stable node depending on the satisfaction of the condition $\kappa+\delta > \omega(1-\rho)$. If coexistence equilibrium P_4 is unstable, therefore equilibrium point P_3 can be a stable node or unstable saddle depending on the satisfaction of the conditions $\kappa+\delta > \omega(1-\rho)$ or $\kappa+\delta < \omega(1-\rho)$, respectively.

To derive the threshold condition for the occurrence of neutral saddle equilibrium (if any) of the coexistence steady-state P_4 when ρ varies is hard due to the complexity of deriving the analytical equation for the three eigenvalues from the characteristic equation in (16). However, saddle-node bifurcation about the coexistence steady-state P_4 will happen if all its feasibility conditions, conditions in (15a) and (19) below

$$\hat{z}(1-\rho-\hat{z})[\sigma\omega+\epsilon(\kappa+\delta)-(1-\rho-2\hat{z})(\eta+\epsilon\omega)]=0, \tag{19}$$

is satisfied. The saddle-node bifurcation occurs at the limit point (LP), which is at the particular value of ρ, such that the previously mentioned conditions hold. Consequently, the characteristic equation of the fishery system (2) in (16) becomes

$$A_1\lambda^3+A_2\lambda^2+A_3\lambda=0. \tag{20}$$

The nonhyperbolic characteristic of the coexistence steady-state P_4, which is a needed condition for saddle-node bifurcation to occur, can be seen in (20). Based on equation (20), the solutions of the three eigenvalues are zero and the other two eigenvalues are negative distinct real numbers since the conditions A_1, A_2 and $A_3 > 0$ and $A_2A_3 > 0$ are satisfied simultaneously.

3.3. Analysis of the global stability for the coexistence steady-state P_4

A mathematical model's global stability implies that, regardless of the initial state, the solutions to a system of differential equations converge to the stable steady-state. This is slightly different from the local stability highlighted in Subsection 3.2. Understanding the stable or unstable interactions among all modeled populations is crucial, that is why we are interested in studying the global stability of the coexistence steady-state P_4. By creating a suitable Lyapunov function, we apply the global stability analysis for the non-trivial or coexistence steady-state P_4. Therefore, we consider Theorem 2.

Theorem 2. *Coexistence equilibrium P_4 in the form of $(\hat{x},\hat{y},\hat{z})$ is globally asymptotically stable in the region of*

$$\frac{y\hat{y}(z-\hat{z})}{\omega[\epsilon y\hat{y}(z-\hat{z})-\eta(x\hat{y}z-\hat{x}y\hat{z})]}>0. \tag{21}$$

Proof. Considering the Lyapunov function for fishery system (2) at coexistence steady-state P_4 be

$$V(x,y,z) = \left((x-\hat{x}) - \hat{x}\ln\frac{x}{\hat{x}}\right) + D_1\left((y-\hat{y}) - \hat{y}\ln\frac{y}{\hat{y}}\right) + D_2\left((z-\hat{z}) - \hat{z}\ln\frac{z}{\hat{z}}\right), \tag{22}$$

where, the positive functions D_1 and D_2 need to be defined in the next steps. It is evident that for any positive values of x, y and z, $V(\hat{x},\hat{y},\hat{z}) = 0$ and $V(x,y,z) > 0$. For the Lyapunov function in (22), its derivative is

$$\begin{aligned}
\frac{dV}{dt} &= \left(\frac{x-\hat{x}}{x}\right)\frac{dx}{dt} + D_1\left(\frac{y-\hat{y}}{y}\right)\frac{dy}{dt} + D_2\left(\frac{z-\hat{z}}{z}\right)\frac{dz}{dt} \\
&= (x-\hat{x})[-(x-\hat{x}) - (z-\hat{z})] + D_1(y-\hat{y})\left[\eta\left(\frac{xz}{y} - \frac{\hat{x}\hat{z}}{\hat{y}}\right) - \epsilon(z-\hat{z})\right] + D_2(z-\hat{z})[\omega(x-\hat{x}) + (y-\hat{y})] \\
&= -\Big\{(x-\hat{x})[(x-\hat{x}) + (z-\hat{z})] - D_1(y-\hat{y})\left[\frac{\eta}{y\hat{y}}(x\hat{y}z - \hat{x}y\hat{z}) - \epsilon(z-\hat{z})\right] - D_2(z-\hat{z})[\omega(x-\hat{x}) + (y-\hat{y})]\Big\} \\
&= -\left\{(x-\hat{x})^2 + (z-\hat{z})[(x-\hat{x})(1-\omega D_2)] + (y-\hat{y})\left[-D_2(z-\hat{z}) - D_1\left(\frac{\eta}{y\hat{y}}(x\hat{y}z - \hat{x}y\hat{z}) - \epsilon(z-\hat{z})\right)\right]\right\}.
\end{aligned}$$

From the latest equation of $\frac{dV}{dt}$, it is clear that the term $(x-\hat{x})^2$ is strictly positive. Hence, we consider both equations $(z-\hat{z})[(x-\hat{x})(1-\omega D_2)] = 0$ and $(y-\hat{y})\left[-D_2(z-\hat{z}) - D_1\left(\frac{\eta}{y\hat{y}}(x\hat{y}z - \hat{x}y\hat{z}) - \epsilon(z-\hat{z})\right)\right] = 0$. Solving both equations simultaneously for D_1 and D_2, we get

$$D_1 = \frac{y\hat{y}(z-\hat{z})}{\omega[\epsilon y\hat{y}(z-\hat{z}) - \eta(x\hat{y}z - \hat{x}y\hat{z})]}, \tag{23}$$

and

$$D_2 = \frac{1}{\omega}. \tag{24}$$

From equation (24), D_2 is strictly positive. If $D_1 > 0$, and we substitute both equations (23) and (24) into the last equation of $\frac{dV}{dt}$, we get

$$\frac{dV}{dt} = -\{(x - \hat{x})^2\}. \tag{25}$$

Hence, from (25), $\frac{dV}{dt} < 0$ in the region in equation (21). This implies a coexistence steady-state P_4 is globally asymptotically stable. It shows that Theorem 2 is legitimate. □

4. Analysis of the Hopf Bifurcation of the Coexistence Equilibrium P_4

Hopf bifurcation (HB) is a periodic solution that arises from the switching behavior in the stability of a coexistence steady-state P_4. This section examines the Hopf bifurcation that occurs around the coexistence steady-state P_4 in response to changes in the prey harvesting (ρ) parameter. Employing the Hopf bifurcation theorem, we verify the presence of the Hopf bifurcation around the coexistence steady-state P_4 concerning that bifurcation parameter.

Theorem 3. *If the condition* $(A_3 - 3A_1\bar{\omega}^2)\left(\frac{dA_4}{d\rho} - \bar{\omega}^2\frac{dA_2}{d\rho}\right) + 2A_2\bar{\omega}^2\frac{dA_3}{d\rho} \neq 0$ *is met. The fishery system (2) experiences a Hopf bifurcation around the coexistence steady-state* P_4 *with respect to the prey harvesting (*ρ*) parameter.*

Proof. Coexistence steady-state P_4's stability depends on the harvesting parameter ρ. The fishery system (2) experiences the Hopf bifurcation if the Jacobian matrix J_{P_4} as in (14) has a pair of purely imaginary eigenvalues and the third eigenvalue has a negative real part. This is in accordance with the Hopf bifurcation theorem used in previous studies [6, 24, 30−32]. The transversality condition $Re\left(\frac{d\lambda}{d\rho}\right)_{\rho=\rho_{HB}} \neq 0$ with respect to ρ as a bifurcation parameter needs to be satisfied for Hopf bifurcation to occur. The Hopf bifurcation point regarding the prey harvesting parameter is shown by the notation ρ_{HB}. Regarding the coexistence steady-state P_4 characteristic equation in (16), the coefficients of the characteristic equation for purely imaginary eigenvalues must meet the requirement $A_2A_3 - A_1A_4 = 0$. It is crucial to note that the other prerequisites are met automatically. To determine the transversality condition that guarantees the occurrence of periodic oscillations via the Hopf bifurcation, Kuang [33] states that we need to choose $\lambda = \pm\, i\bar{\omega}$ be a pair of purely

imaginary eigenvalues with respect to ρ_{HB}. By differentiating the characteristic equation in (16) concerning ρ, we can now get

$$\frac{d\lambda}{d\rho} = -\frac{\lambda^2 \frac{dA_2}{d\rho} + \lambda \frac{dA_3}{d\rho} + \frac{dA_4}{d\rho}}{3A_1\lambda^2 + 2\lambda A_2 + A_3}.$$

Therefore,

$$\left(\frac{d\big(Re(\lambda)\big)}{d\rho}\right)_{\lambda=i\bar{\omega}} = Re\left(-\frac{\lambda^2 \frac{dA_2}{d\rho} + \lambda \frac{dA_3}{d\rho} + \frac{dA_4}{d\rho}}{3A_1\lambda^2 + 2\lambda A_2 + A_3}\right)_{\lambda=i\bar{\omega}}$$

$$= Re\left(-\frac{(i\bar{\omega})^2 \frac{dA_2}{d\rho} + i\bar{\omega} \frac{dA_3}{d\rho} + \frac{dA_4}{d\rho}}{3A_1(i\bar{\omega})^2 + 2i\bar{\omega}A_2 + A_3}\right).$$

By solving the latest equation above, we acquired

$$\left(\frac{d\big(Re(\lambda)\big)}{d\rho}\right)_{\lambda=i\bar{\omega}} = -\frac{(A_3 - 3A_1\bar{\omega}^2)\left(\frac{dA_4}{d\rho} - \bar{\omega}^2 \frac{dA_2}{d\rho}\right) + 2A_2\bar{\omega}^2 \frac{dA_3}{d\rho}}{(A_3 - 3A_1\bar{\omega}^2)^2 + (2A_2\bar{\omega})^2}. \quad (26)$$

Hence, if the condition $(A_3 - 3A_1\bar{\omega}^2)\left(\frac{dA_4}{d\rho} - \bar{\omega}^2 \frac{dA_2}{d\rho}\right) + 2A_2\bar{\omega}^2 \frac{dA_3}{d\rho} \neq 0$ in equation (26) is met. Consequently, the fishery system (2) experiences Hopf bifurcation with respect to the bifurcation parameter ρ. The Theorem 3 has been proven. □

5. RESULTS AND ANALYSIS OF BIFURCATION

In this section, we implement numerical simulations to analyze the impacts of prey harvesting, which is considered a bifurcation parameter, on the dynamical behavior of the extreme fishery system (2) by using Maple 18, XPPAUT and MATLAB R2021a softwares [34−36]. A set of hypothetical parameter values $\rho = 0.1$, $\omega = 0.3$, $\kappa = 0.05$, $\delta = 0.2$, $\eta = 0.3$, $\sigma = 0.2$ and $\epsilon = 0.1$ is chosen to show the bifurcation results due to the hardly available primary data in simulating our fishery model.

5.1. Prey harvesting (ρ) as a bifurcation parameter

The bifurcation diagrams of prey (x), prey carrion biomass (y) and apex facultative scavenger (z) versus prey harvesting (ρ) are shown in Fig. 1. In all bifurcation diagrams, the blue solid lines and curves represent stable steady-states, the red dashed-dotted lines and curves represent unstable steady-states, and the green curve represents the Hopf locus.

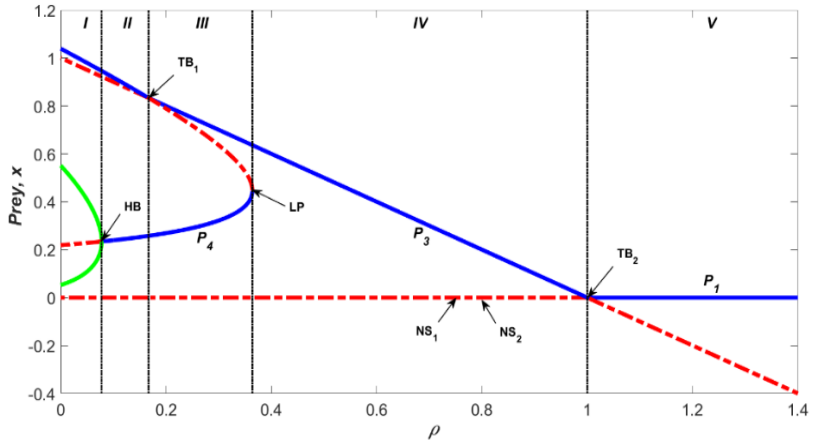

(a)

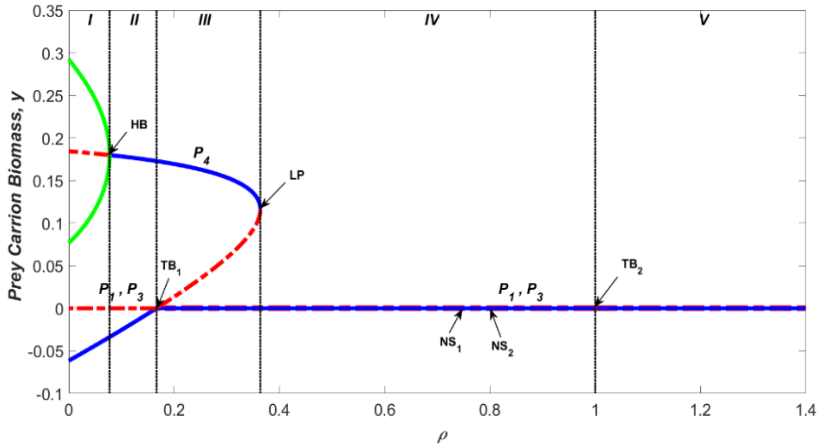

(b)

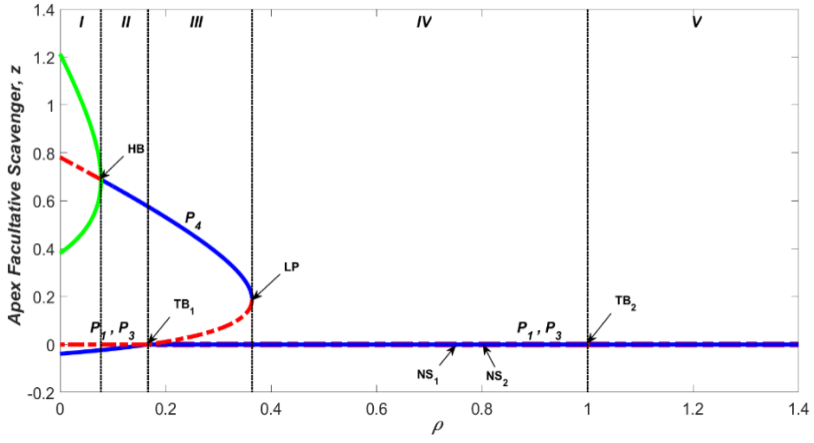

(c)

Figure 1: Bifurcation diagrams of fishery system (2) with varying values of prey harvesting parameter, ρ for (a) prey, x, (b) prey carrion biomass, y and (c) apex facultative scavenger, z, respectively.

Based on Fig. 1 in Region I, which is $0 \leq \rho < 0.0774$, the coexistence steady-state P_4 is unstable as shown in the red dashed-dotted curve. The steady-state is unstable due to the existence of periodic oscillations around it, which is illustrated by an open green loop that appears from a Hopf bifurcation (HB) point at $\rho_{HB} = 0.0774$. By using the characteristic equation (16), we can determine the HB point with respect to the prey harvesting parameter by considering the requirement $A_2A_3 - A_1A_4 = 0$. By letting parameter ρ be unknown, we can solve for ρ and obtain one HB point, which is $\rho_{HB} = 0.0774$. Then, we solve the characteristic equation (16) and acquire three eigenvalues, which are $\lambda_{1,2} = \pm 0.2744\text{i}$ and $\lambda_3 = -0.5029$. The term $\bar{\omega}$ in the transversality condition in (26) refers to the real numbers of purely imaginary eigenvalues, in this case $\bar{\omega} = \pm 0.2744$, getting from $\lambda_{1,2}$. Upon replacing all term values in the transversality condition (26), we obtain $Re\left(\frac{d\lambda}{d\rho}\right)_{\rho_{HB}=0.0774} = -0.1796$, therefore proving Theorem 3. The periodic oscillations grow more when ρ decreases due to the impact of lower prey harvesting levels on the extreme growth of apex facultative scavengers. The amplitudes of periodic oscillations at their maximum and minimum points are represented by the higher and lower parts of the open green loop, respectively. These results relevantly occurred in the fishery system, where they can also be seen from previous research [17, 37]. Jana and Panja [17] investigate the interaction of prey, predator and scavenger populations by assuming predator and scavenger quadratic harvesting as bifurcation parameters. Besides, Savoca et al. [37] analyzed the effects of the hermit crab (predator) death rate on the stability of the Messina beachrock pools system in the presence of a top snail (prey) population via bifurcation analysis.

From Fig. 1, in Region II ($0.0774 < \rho \leq 0.1667$), where $\rho = 0.1667$ is the first transcritical bifurcation point (TB_1) derived by considering equation (13). At the TB_1 point, the initially stable unfeasible coexistence steady-state P_4 (blue solid curve) changes to the unstable feasible coexistence steady-state P_4 (red dashed-dotted curve), whereas the steady-state P_3 changes from unstable (red dashed-dotted line) to stable (blue solid line). In Region II, the coexistence equilibrium P_4 is stable, as shown in the blue solid curve due to the decreasing level of apex facultative scavengers preying on prey. The increasing level of prey harvesting causes both prey carrion biomass and apex facultative scavengers to decrease in their densities in the fishery system, as illustrated in Figs. 1(b) and 1(c), respectively. This situation will reduce the dominance of the apex facultative scavenger population in the fishery system. This condition is preferable where all interacting species persist in their harmonious interaction. On the other hand, in the range of $0 \leq$

$\rho < 0.1667$, the unfeasible coexistence steady-state P_4 is stable, as illustrated in the blue solid curve, but we ignore it because it is not biologically relevant.

Based on Region III ($0.1667 < \rho < 0.3637909870$), where $\rho = 0.3637909870$ is the limit point (LP), this can be verified through the satisfaction of all feasibility conditions of the coexistence equilibrium P_4 in (5a)− (5c) and conditions in equations (15a) and (19). In Region III of Fig. 1, the curve for the coexistence steady-state P_4 has two types of stability, which are stable steady-states (blue solid curve) and unstable steady-states (red dashed-dotted curve). By our numerical simulation, to show the existence of the saddle-node bifurcation at the LP point, we consider the values of ρ which are before and close to the LP point, to see the changes in the values of eigenvalues for the coexistence steady-states P_4 where their hyperbolic characteristics gradually disappear when approaching limit point. Based on Table 1 below, when $\rho = 0.3600$ associated eigenvalues for the coexistence steady-state (0.4112, 0.1266, 0.2288) of the blue solid curve are $\lambda_1 = -0.0307$, $\lambda_2 = -0.1792$ and $\lambda_3 = -0.4241$, while the coexistence steady-state (0.4863, 0.1041, 0.1537) of the red dashed-dotted curve having the eigenvalues of $\lambda_1 = 0.0157$, $\lambda_2 = -0.2536$ and $\lambda_3 = -0.4638$. Based on the analysis of the eigenvalues [30, 38], we can conclude that the coexistence steady-state (0.4112, 0.1266, 0.2288) is a stable node, while (0.4863, 0.1041, 0.1537) is an unstable saddle point. Refer to Table 1, for more increasing values of ρ ($0.3600 < \rho < 0.3637909870$), the hyperbolic characteristics of the coexistence steady-states P_4 gradually disappear, which is shown by the values of λ_1, which are gradually approaching 0.

The saddle-node bifurcation about the coexistence steady-state P_4 occurs at the limit or turning point, where the initially two distinct stability of coexistence steady-states, which are stable node and unstable saddle collide and annihilate each other at the LP point. Substituting the value of $\rho = 0.3637909870$ into the characteristic equation (20), the eigenvalues obtained for saddle-node equilibrium point (0.4469, 0.1159, 0.1893) are $\lambda_1 = 0$, $\lambda_2 = -0.2290$ and $\lambda_3 = -0.4368$, which is the non-hyperbolic characteristic of coexistence steady-state P_4 is shown. The non-hyperbolic characteristic of steady-state is a required condition for the saddle-node bifurcation to occur [39, 40]. Besides, the bistability phenomenon of the steady-states occurs in this region, where both the coexistence steady-state P_4 and the equilibrium of only prey presence P_3 are stable. Depending on the initial population sizes of interacting populations and the values of the prey harvesting rate, the solutions of the fishery model will converge to one of the stable steady-states.

Table 1: The types of stability for the coexistence steady-states P_4 at ρ = 0.3600, 0.3610, 0.3620, 0.3630 and 0.3637.

Prey harvesting (ρ) values	**Coexistence steady-states P_4**	**Eigenvalues**	**Types of stability of the coexistence steady-states P_4**
0.3600	(0.4112, 0.1266, 0.2288)	$\lambda_1 = -0.0307, \lambda_2 = -0.1792, \lambda_3 = -0.4241$	Stable node
	(0.4863, 0.1041, 0.1537)	$\lambda_1 = 0.0157, \lambda_2 = -0.2536, \lambda_3 = -0.4638$	Unstable saddle
0.3610	(0.4161, 0.1252, 0.2229)	$\lambda_1 = -0.0246, \lambda_2 = -0.1886, \lambda_3 = -0.4252$	Stable node
	(0.4805, 0.1058, 0.1585)	$\lambda_1 = 0.0140, \lambda_2 = -0.2513, \lambda_3 = -0.4591$	Unstable saddle
0.3620	(0.4220, 0.1234, 0.2160)	$\lambda_1 = -0.0183, \lambda_2 = -0.1986, \lambda_3 = -0.4267$	Stable node
	(0.4736, 0.1079, 0.1644)	$\lambda_1 = 0.0118, \lambda_2 = -0.2480, \lambda_3 = -0.4538$	Unstable saddle
0.3630	(0.4301, 0.1210, 0.2069)	$\lambda_1 = -0.0112, \lambda_2 = -0.2102, \lambda_3 = -0.4294$	Stable node
	(0.4644, 0.1107, 0.1726)	$\lambda_1 = 0.0083, \lambda_2 = -0.2427, \lambda_3 = -0.4473$	Unstable saddle
0.3637	(0.4411, 0.1177, 0.1952)	$\lambda_1 = -0.0034, \lambda_2 = -0.2232, \lambda_3 = -0.4340$	Stable node
	(0.4527, 0.1142, 0.1836)	$\lambda_1 = 0.0031, \lambda_2 = -0.2341, \lambda_3 = -0.4400$	Unstable saddle

After that, in Region IV which is $0.3637909870 \leq \rho < 1.0$, where $\rho = 1.0$ is a second transcritical bifurcation (TB_2) value. In this region, steady-state P_3 is stable. The growth of the prey population is decreasing as visualized in Fig. 1(a), while both prey carrion biomass and the apex facultative scavenger population are absent in the fishery system as shown in Figs. 1(b) and 1(c), respectively, because of the increasing harvesting rate level of prey. Predation interaction between apex facultative scavengers and prey does not happen, thus making prey carrion unavailable in the fishery system. Apex facultative scavengers are driven to extinction in the fishery system because of harvesting activity on them and predation pressure from their apex predators that compete for the same food (prey) that is driven by the decreasing level of prey population density. However, in this present research, we do not mathematically model the predation and competition interactions between apex facultative scavengers and their apex predators, but we considered that the natural death rate of apex facultative scavengers is contributed by these factors. Moreover, the limitation of the apex facultative scavenger population alternative foods in an extreme fishery system can also cause extirpation in their population. In this region, first neutral saddle point (NS_1) occurs at $\rho = 0.7500$, and second neutral saddle point (NS_2) at $\rho = 0.8000$ which can be verified by considering equations (7) and (8), where the corresponding eigenvalues of the neutral saddle equilibrium P_1 (red dashed-dotted line) are $\lambda_{1,2} = \pm 0.2500$, $\lambda_3 = -0.2000$ and $\lambda_{1,2} = \pm 0.2000$, $\lambda_3 = -0.2500$, respectively. The sum of $\lambda_{1,2}$ is zero. The value of $TB_2 = 1.0$ indicates the transition of the stability of equilibrium P_3, which is from stable (blue solid line) to unstable (red dashed-dotted line), while extinction equilibrium P_1 changes from unstable to stable.

Lastly, in Region V where $\rho > 1.0$, the fishery system collapses due to prey overharvesting and the extreme conditions in the fishery system, where all interacting populations are extinct, which is steady-state P_1 is stable. The harvesting rate of prey is impactful on the stability of the extreme fishery system (2) due to its critical conditions, where carnivorous apex facultative scavengers only depend on prey and prey carrion to survive.

5.1.1. Time series plots for each region of the bifurcation diagram

In this part, we visualized the graphs of interacting populations versus time at particular values of prey harvesting, ρ for each region of bifurcation diagrams in Fig. 1. Through this part, we can observe and analyze the growth patterns of the modeled populations from the fishery model (2) concerning time.

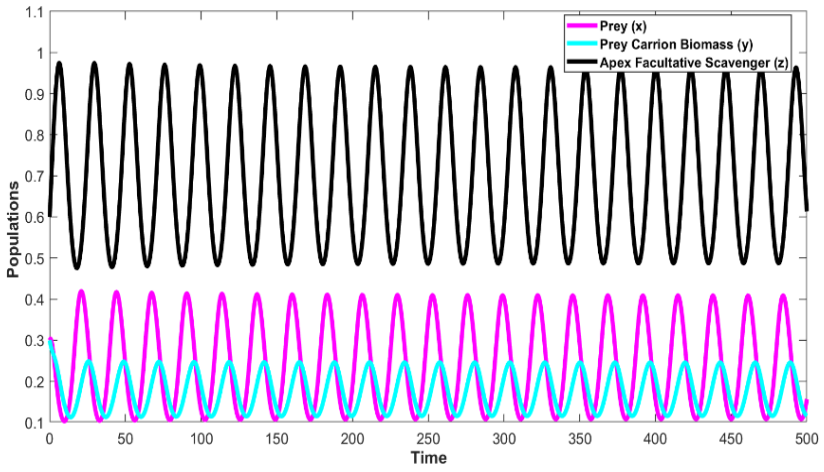

Figure 2: Time series plot of fishery system (2) with initial condition of $(x_0, y_0, z_0) = (0.3,0.3.0.6)$ at $\rho = 0.05$ (Region I).

In Fig. 2, the graph of prey (x), prey carrion biomass (y) and apex facultative scavenger (z) versus time at $\rho = 0.05$, which is in the range of Region I is plotted. The apex facultative scavenger population is dominating the fishery system due to the low rate of prey harvesting, as seen in Figs. 1 and 2. This is because they have access to an abundance of food sources, such as live prey and prey carrion. That situation makes the fishery system's coexistence steady-state P_4 unstable. The periodic oscillations occur around the unstable coexistence steady-state (0.2282, 0.1815, 0.7218), which is not a good and undesirable condition in the fishery system due to the fluctuation in the population densities of x, y and z. According to previous research by Hussin et al. [6] and Hussin, Embong and Noor [41], the periodic oscillations around the unstable coexistence steady-states of their population models also appear due to the high scavenging rate of scavengers and high time delay in Holling type II functional response, respectively. The large amount of scavenged predator carcasses ensures the domination of scavengers in the fishery system, which can have a bad effect on the stability of the fishery system [6]. On the other hand, the high time lag in predator response function disturbs the previously stable prey-predator interaction [41].

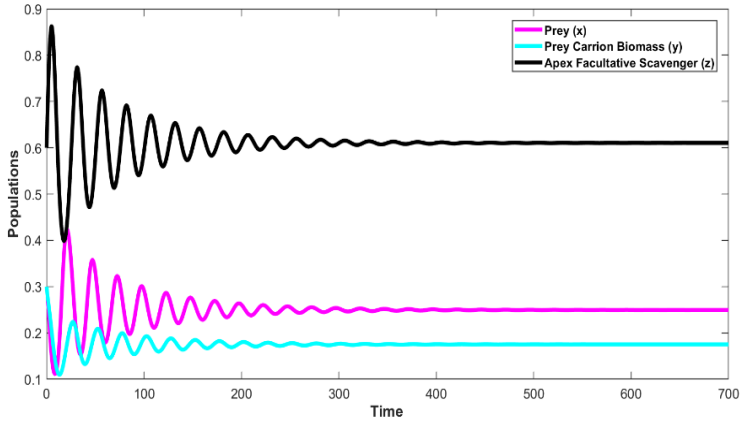

Figure 3: Time series plot of fishery system (2) with initial condition of $(x_0, y_0, z_0) = (0.3,0.3.0.6)$ at $\rho = 0.14$ (Region II).

In Fig. 3, the graph of all interacting populations versus time at $\rho = 0.14$ (Region II) is illustrated. Initially, harvesting operation of prey and predation effects on prey from apex facultative scavengers cause the depletion in the number of prey population in the fishery system. Prey carrion biomasses decrease due to the scavenging effect of apex facultative scavengers. The growth of apex facultative scavengers is increasing due to the sufficient food sources from the live prey and prey carrion. After that, the population number of apex facultative scavengers alternately decreases and increases, which is opposite to the growth of prey and prey carrion biomass formation, which alternately increases and decreases. From the initial period, prey carrion biomass density slowly decreases and increases as compared to prey due to the positive and negative effects of apex facultative scavengers on carrion formation through predation interaction with prey and the loss rate of prey carrion during scavenging, respectively. Over time, all interacting populations converge to their equilibrium state (0.2496, 0.1751, 0.6104).

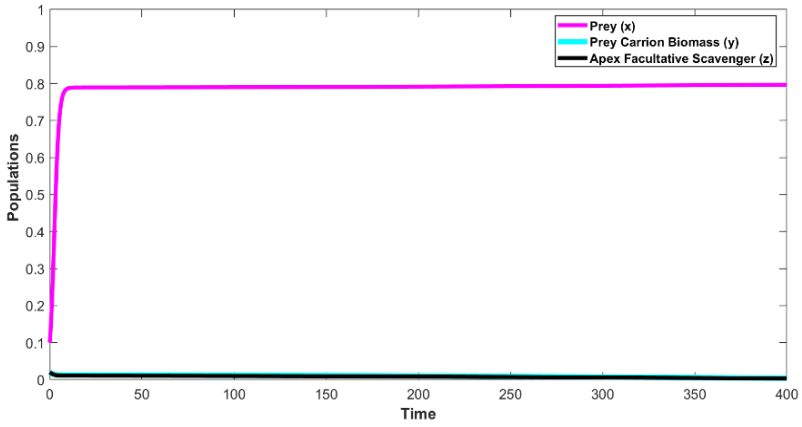

(a)

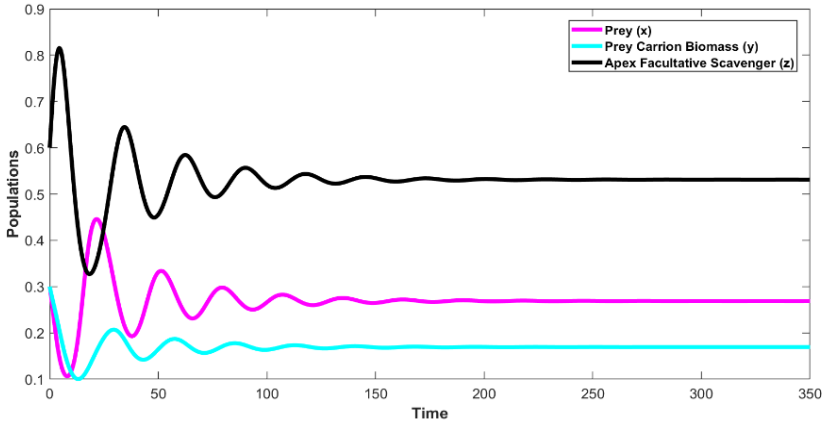

(b)

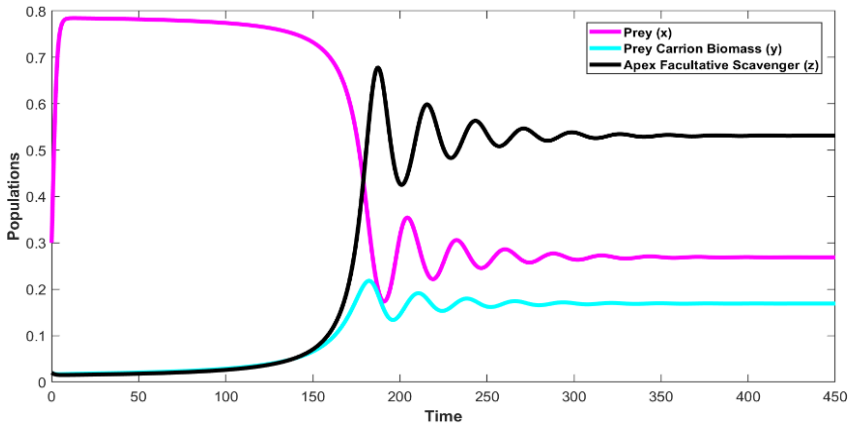

(c)

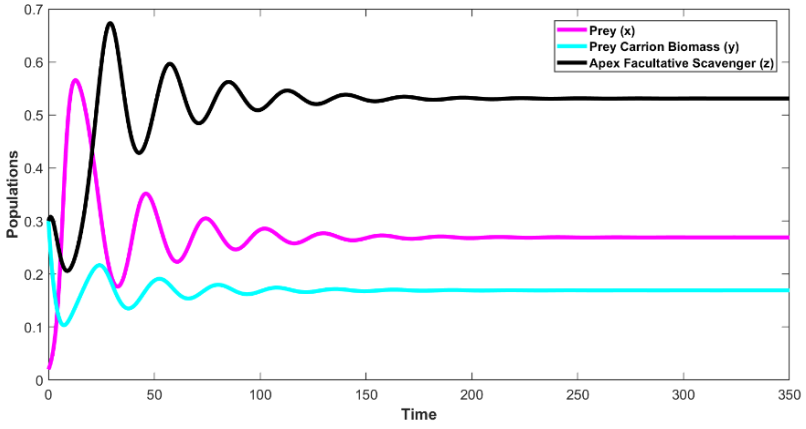

(d)

Figure 4: Time series plots of fishery system (2) with $\rho = 0.2$ (Region III) at initial conditions of (a) $(x_0, y_0, z_0) = (0.1,0.02,0.02)$, (b) $(x_0, y_0, z_0) = (0.3,0.3,0.6)$, (c) $(x_0, y_0, z_0) = (0.3,0.02,0.02)$ and (d) $(x_0, y_0, z_0) = (0.02,0.3,0.3)$, respectively.

We visualized the graph of interacting populations versus time at $\rho = 0.2$ (Region III), and its corresponding steady-states can be (0.8,0,0) as P_3 and (0.2690, 0.1693, 0.5310) as P_4. Based on the fishery system (2), the densities of prey carrion (y) and apex facultative scavenger (z) depend on prey population (x). This is because prey act as sources of food for apex facultative scavengers in terms of their live population and carrion biomass. If the initial conditions for x, y and z are low, which is (0.1, 0.02, 0.02), then the steady-state P_3 is stable, as shown in Fig. 4(a). This is because the small number of the initial population of prey is unable to support the growth of the initially small population number of apex facultative scavengers, thus causing the extirpation of the apex facultative scavenger population and the non-existence of prey carrion. No predation interaction between prey and apex facultative scavengers will cause no formation of prey carrion. In Fig. 4(a), when prey carrion and apex facultative scavenger approach zero population densities due to the indirect effect of prey harvesting and their low initial population densities, prey drastically increases, and after that, they converge to an equilibrium state (0.8,0,0). The prey population survives due to no threat from the apex facultative scavenger population.

According to Fig. 4(b), the high initial populations for x, y and z which is (0.3,0.3,0.6), guarantee the stability of coexistence steady-state P_4. The number of periodic oscillations of interacting populations versus time in Fig. 4(b) is smaller than in Fig. 3, due to the lower dominance of apex facultative scavengers in the fishery system as compared to Fig. 3 because of higher prey harvesting level. The value of $\rho = 0.2$ does not decrease the growth of prey due to their large initial population number. However, the growth of apex facultative scavengers and the formation of prey carrion are indirectly affected by prey harvesting. This situation will facilitate the convergence of interacting populations to their equilibrium state. Based on Fig. 4(c), the low initial values of y and z and high value of x such as (0.3, 0.02, 0.02) make the coexistence steady-state P_4 stable due to the sufficient food sources from live prey and remaining prey carrion to apex facultative scavengers' growth. In Fig. 4(c), initially, the growth of prey is fast and close to $x = 0.8$ due to the less predation effect from apex facultative scavengers. The population density of apex facultative scavengers and prey carrion approaches 0. After that, the growth of apex facultative scavengers and the formation of prey carrion from dead prey increased because of food sources contributed by prey to apex facultative scavengers. The further enhancement in the population of apex facultative scavengers and prey carrion formation causes a depletion in the number of prey population and the appearance of periodic oscillations. Over time, all interacting populations converge to their equilibrium state.

Regarding Fig. 4(d), the large initial numbers of y and z and the small initial number of x which is (0.02, 0.3, 0.3), make the coexistence steady-state P_4 stable. This is because apex facultative scavengers can survive in the fishery system with their initially high population and food source from prey carrion. Initially, for a small period, the population of apex facultative scavengers increased due to the sufficient food sources from prey carrion and prey. Then, when prey carrion further drastically decreases and the population number of prey is small due to harvesting and their small initial population number, apex facultative scavengers start to decrease. After that, the population density of prey increases. A further increase in the population of prey triggers the growth of apex facultative scavengers and the formation of prey carrion. Next, the continuous growth in the population number of apex facultative scavengers and the density of prey carrion cause a reduction in the growth of prey. Periodic oscillations occur when prey and apex facultative scavengers oppositely increase and decrease. The formation of prey carrion follows apex facultative scavengers' growth as time increases. Over time, all populations converge to their equilibrium state.

Based on the analysis of our fishery model, if the value of $\rho < 0.2$ and in the range of Region III, for example $\rho = 0.17$, and apply the initial condition (0.1, 0.02, 0.02), which has been considered a low initial condition value for the time series plot when $\rho = 0.2$ as in Fig. 4(a), the coexistence steady state P_4 becomes stable as shown in Fig. 5. This is because the low prey harvesting rate can maintain the coexistence of interacting populations in the fishery system. This situation shows that the rate of prey harvesting plays an important role in avoiding the non-coexistence state of interacting populations.

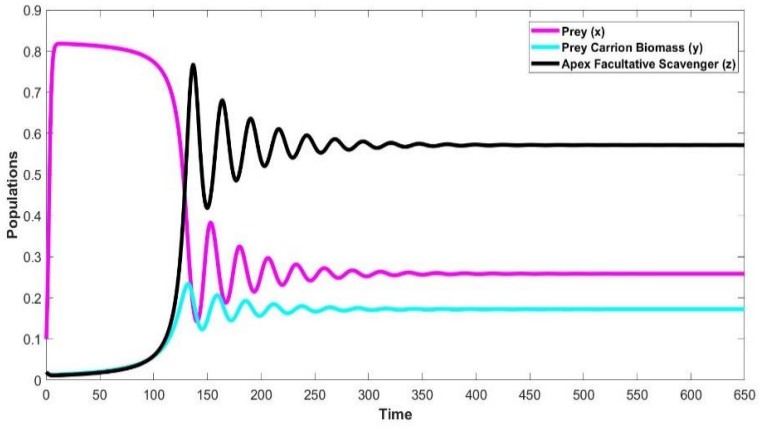

Figure 5: Time series plot of fishery system (2) with initial condition of $(x_0, y_0, z_0) = (0.1,0.02.0.02)$ at $\rho = 0.17$ (Region III).

Based on Fig. 5, initially, the growth of apex facultative scavengers and the formation of prey carrion approaches 0, this is due to their low initial condition values and the indirect effect of prey harvesting. For a short period, the growth of prey is drastically increased because of less threat from apex facultative scavengers. After that, the growth of apex facultative scavengers and prey carrion formation increases, whereas prey decreases due to the food source contributed by prey. Next, the growth of apex facultative scavengers and prey carrion formation drastically increase, whereas prey sharply decreases. The apex facultative scavenger population gets sufficient food sources from prey and prey carrion. The fluctuation in the population densities of interacting populations occurs and over time, converges to their equilibrium state (0.2586, 0.1724, 0.5714).

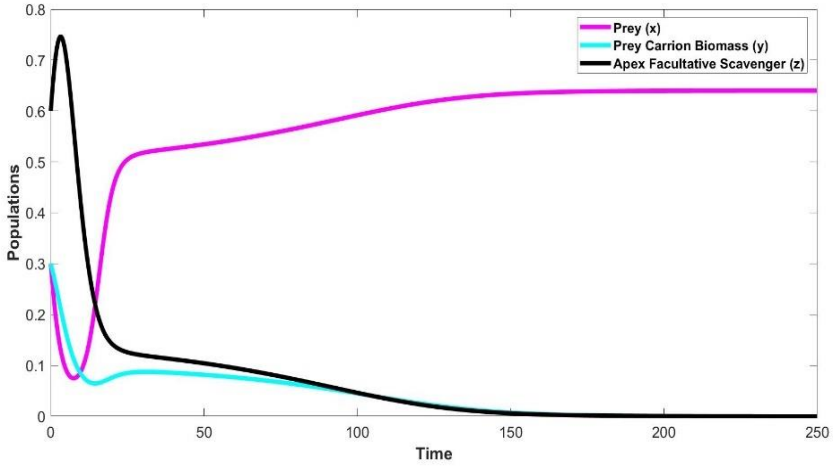

Figure 6: Time series plot of fishery system (2) with initial condition of $(x_0, y_0, z_0) = (0.3,0.3,0.6)$ at $\rho = 0.36$ (Region III).

Besides, for the value of $\rho > 0.2$ and in the range of Region III, for instance $\rho = 0.36$, the high initial condition (0.3, 0.3, 0.6) that we applied in Fig. 4(b) makes the steady-state P_3 stable as shown in Fig. 6. This is because the high prey harvesting rate can cause extinction states for both apex facultative scavenger population and prey carrion biomass. The growth of apex facultative scavengers and prey carrion formation fundamentally depends on prey population density. According to Fig. 6, initially, the growth of apex facultative scavengers increases because of their high initial condition and their sufficient food sources from prey and prey carrion. The growth of prey and their carrion formation decrease because of predation and scavenging impacts from apex facultative scavengers, respectively. After that, the growth of apex facultative scavengers starts to decrease due to the further reduction in their sources of food. Apex facultative scavenger populations continuously decreased, resulting in an enhancement of the prey population. However,

prey carrion biomass formation continues to decrease because of a reduction in the apex facultative scavenger population, which can produce prey carrion. For increasing time, the prey carrion biomass increases because of less scavenging impact from apex facultative scavengers. The further reduction in the apex facultative scavenger population makes the prey carrion biomass density decrease again due to the same reason as stated before. The growth of prey is increasing. Over time, all modeled populations converge to their equilibrium state (0.6400, 0, 0).

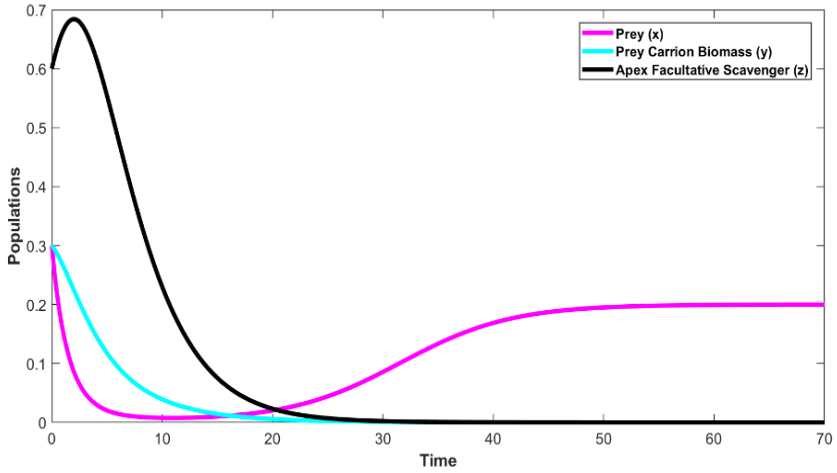

Figure 7: Time series plot of fishery system (2) with initial condition of $(x_0, y_0, z_0) = (0.3,0.3.0.6)$ at $\rho = 0.8$ (Region IV).

Based on Fig. 7, the graph of x, y and z versus time is illustrated by considering $\rho = 0.8$ (Region IV). In the earlier period, the growth of prey decreased due to the harvesting and predation effects of increasing apex facultative scavengers, whereas prey carrion biomass density slowly decreased due to the positive and negative effects of apex facultative scavengers increasing growth. Based on the fishery system (2), the prey carrion biomass density depends on the density of caught prey that is converted into carrion. The more apex facultative scavengers that can form prey carrion, the higher the density of prey carrion. However, the high scavenging rate of prey carrion may reduce their density. Next, the growth of apex facultative scavengers decreases due to the further decrease in their sources of food which are approaching 0. For a longer period, the population of prey increases and converges to their equilibrium population $x = 0.2$ due to no threat from apex facultative scavengers. The apex facultative scavenger population is extinct because of the loss of their source of food from prey carrion and the indirect effect of prey harvesting. This situation shows that prey carrion is very important for apex facultative scavengers' growth.

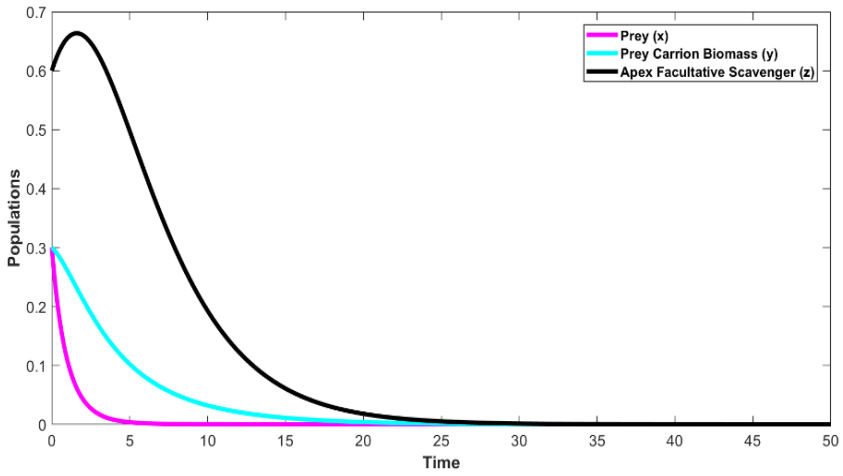

Figure 8: Time series plot of fishery system (2) with initial condition of $(x_0, y_0, z_0) = (0.3,0.3.0.6)$ at $\rho = 1.2$ (Region V).

In Fig. 8, we illustrate the pattern of growth for the interacting populations versus time when the prey harvesting rate is extremely high, which is $\rho = 1.2$. The growth of interacting populations in Figs. 7 and 8 are quite similar. However, in this figure, because of prey overharvesting, the fishery system (2) collapsed. This situation shows that prey overexploitation is harmful to the fishery system.

6. Conclusions and Discussions

In this paper, we have formulated a new extreme fishery model with the presence of prey and apex facultative scavenger harvesting. Our objective is to analyze the prey harvesting impacts on the stability of the extreme fishery system via bifurcation analysis. The fishery system is considered an extreme condition because carnivorous apex facultative scavengers totally depend on their main food preferences, which are the vertebrate marine prey and their carrion as sources of food. Without the existence of prey, apex facultative scavengers may extirpate due to the limitations of their alternative foods like invertebrate marine animals. Moreover, the habitat conditions may reduce the density of prey carrion biomass by accelerating the decomposition of prey carrion in the fishery system. This situation triggers competition between apex facultative scavengers and their competitors due to the scarcity of food sources.

The Jacobian matrices and their associated eigenvalues have been computed to analyze the local stability of the steady-states of the fishery system (2). The Lyapunov function has been applied to analyze the global stability of the coexistence steady-state. Prey harvesting (ρ) is considered a

bifurcation parameter. The threshold conditions are computed and evaluated for the occurrence of local bifurcations which are saddle-node bifurcation and transcritical bifurcation (TB) at the steady-states of the fishery system (2). To prove the existence of Hopf bifurcation (HB), which is also a type of local bifurcation, the Hopf bifurcation theorem has been used. The bifurcation analysis indicates that the extreme fishery model's dynamical behaviors are significantly influenced by prey harvesting activities.

According to the bifurcation diagrams in Fig. 1, at the low level of prey harvesting rates, which is in the range of Region I, the periodic oscillations around the unstable coexistence steady-state P_4 appear through the HB point. This is due to the dominance of apex facultative scavengers in the fishery system that acquired oversufficient food sources from prey and prey carrion. Next, at the intermediate level of prey harvesting rates, which is in the range of Region II, the coexistence steady-state P_4 is stable because of the reduction of both prey carrion and apex facultative scavenger population densities due to the indirect effect of prey harvesting. At the range of Region III, where prey harvesting rates are at a high level, the bistability phenomenon appears, where both equilibrium P_3 and P_4 are stable depending on the initial conditions of interacting populations and prey harvesting rate values. The low initial condition values for all interacting populations and the low prey harvesting rate (in the range of Region III) give rise to the stability of coexistence equilibrium P_4. As opposed to that, the high prey harvesting rate (in the range of Region III) can make apex facultative scavengers extinct and no prey carrion biomass formation even though the initial condition values of modeled populations are high. This is because the level of prey harvesting plays an important role in determining the prey population density level, which acts as the main food source for apex facultative scavengers. Besides, in this region, the saddle-node bifurcation occurs at the LP point, where the initially two distinct stabilities of coexistence steady-states P_4 collide and annihilate each other.

For further increases in prey harvesting rates, which are in the range of Region IV, equilibrium P_3 is stable because of the extirpation of apex facultative scavengers due to their lost opportunity to scavenge prey carrion and the reduction of prey population. At the extremely high level of prey harvesting (Region V), the extinction equilibrium P_1 is stable, where all interacting populations vanish in the fishery system. Therefore, we can conclude that the rate of prey harvesting (ρ) is crucial to the stability of the extreme fishery system (2). The good condition is when all interacting populations persist together with their stable interaction in the fishery system, which is at the intermediate level of ρ values. Because fisheries may produce food for people and a means of

revenue for fishermen and the nation, it is imperative that the system remain stable. The preservation of threatened aquatic life can be implemented by providing marine protected areas for them and applying good harvesting practices that can maintain the sustainability of harvested marine life.

ACKNOWLEDGEMENTS

The authors would like to thank the Research Management Center (RMC), Universiti Tun Hussein Onn Malaysia for the supported Research Enhancement Graduate Grant (RE-GG) with grant code Q080 to publish this present research. Communication of this research is also made possible through monetary assistance from Universiti Tun Hussein Onn Malaysia and the UTHM Publisher's Office via Publication Fund E15216. Besides, the authors would also acknowledge the Ministry of Higher Education Malaysia and Research Management Center-UTM, Universiti Teknologi Malaysia (UTM) for the funding under UTM Encouragement Research (UTMER) through vote number Q.J130000.3854.31J08.

CONFLICT OF INTERESTS

The authors declare that there is no conflict of interests.

REFERENCES

[1] J. Depestele, J. Feekings, D.G. Reid, et al. The impact of fisheries discards on scavengers in the sea, in: S.S. Uhlmann, C. Ulrich, S.J. Kennelly (Eds.), The European Landing Obligation, Springer International Publishing, Cham, 2019: pp. 129–162. https://doi.org/10.1007/978-3-030-03308-8_7.

[2] J.C. Carrier, J.A. Musick, M.R. Heithaus, eds., Biology of sharks and their relatives, CRC Press, 2004. https://doi.org/10.1201/9780203491317.

[3] J.E. Higuera-Rivas, E.M. Hoyos-Padilla, F.R. Elorriaga-Verplancken, et al. Orcas (Orcinus orca) use different strategies to prey on rays in the Gulf of California, Aquat. Mamm. 49 (2023), 7–18. https://doi.org/10.1578/AM.49.1.2023.7.

[4] F.G. Carey, J.W. Kanwisher, O. Brazier, et al. Temperature and activities of a white shark, carcharodon carcharias, Copeia 1982 (1982), 254-260. https://doi.org/10.2307/1444603.

[5] C. Mackey, C. Kribs, Can scavengers save zebras from anthrax? A modeling study, Infect. Dis. Model. 6 (2021), 56–74. https://doi.org/10.1016/j.idm.2020.10.016.

[6] W.N.W. Hussin, H.M. Safuan, T.K. Ang, et al. The impacts of scavenging on the prey-predator-scavenger fishery model in the existence of harvesting and toxin, J. Adv. Res. Appl. Sci. Eng. Technol. 31 (2023) 254–270. https://doi.org/10.37934/araset.31.1.254270.

[7] B.M. Yagnesh, C.F. Durga, M.D. Raj, et al. Importance of sharks in ocean ecosystem, J. Entomol. Zool. Stud. 8 (2020), 611-613.

[8] K. Kelleher, Discards in the world's marine fisheries: an update, Food and Agriculture Organization of the United Nations, Rome, 2005.

[9] D. Zeller, T. Cashion, M. Palomares, et al. Global marine fisheries discards: A synthesis of reconstructed data, Fish Fish. 19 (2017), 30–39. https://doi.org/10.1111/faf.12233.

[10] W.A. Karp, M. Breen, L. Borges, et al. Strategies used throughout the world to manage fisheries discards – lessons for implementation of the EU landing obligation, in: S.S. Uhlmann, C. Ulrich, S.J. Kennelly (Eds.), The European Landing Obligation, Springer International Publishing, Cham, 2019: pp. 3–26. https://doi.org/10.1007/978-3-030-03308-8_1.

[11] W.W.L. Cheung, T.L. Frölicher, V.W.Y. Lam, et al. Marine high temperature extremes amplify the impacts of climate change on fish and fisheries, Sci. Adv. 7 (2021), eabh0895. https://doi.org/10.1126/sciadv.abh0895.

[12] R. Nero, M. Cook, J. Reneker, et al. Decomposition of Kemp's ridley (Lepidochelys kempii) and green (Chelonia mydas) sea turtle carcasses and its application to backtrack modeling of beach strandings, Endang. Species. Res. 47 (2022), 29–47. https://doi.org/10.3354/esr01164.

[13] C. Zhou, R.W. Byard, Factors and processes causing accelerated decomposition in human cadavers – An overview, J. Forensic Leg. Med. 18 (2011), 6–9. https://doi.org/10.1016/j.jflm.2010.10.003.

[14] D.O. Carter, A. Orimoto, C.A. Gutierrez, et al. A synthesis of carcass decomposition studies conducted at a tropical (Aw) taphonomy facility: 2013–2022, Forensic Sci. Int. Synergy 7 (2023), 100345. https://doi.org/10.1016/j.fsisyn.2023.100345.

[15] C.J. O'Bryan, M.H. Holden, J.E.M. Watson, The mesoscavenger release hypothesis and implications for ecosystem and human well‐being, Ecol. Lett. 22 (2019), 1340-1348. https://doi.org/10.1111/ele.13288.

[16] J.P. Mellard, S. Hamel, J. Henden, et al. Effect of scavenging on predation in a food web, Ecol. Evol. 11 (2021), 6742–6765. https://doi.org/10.1002/ece3.7525.

[17] D.K. Jana, P. Panja, Effects of supplying additional food for a scavenger species in a prey-predator-scavenger model with quadratic harvesting, Int. J. Model. Simul. 43 (2023), 250–264. https://doi.org/10.1080/02286203.2022.2065658.

[18] S.D. Zawka, T.T. Melese, Dynamics and optimal harvesting of prey–predator in a polluted environment in the presence of scavenger and pollution control, Math. Open 02 (2023), 2350004. https://doi.org/10.1142/S2811007223500049.

[19] L. dos Anjos, Population modelling insights of extinct environments: the case of the Kem Kem palaeocommunity, preprint, (2021). https://doi.org/10.1101/2021.09.07.459352.

[20] M.H. Holden, J. Lockyer, Poacher-population dynamics when legal trade of naturally deceased organisms funds

anti-poaching enforcement, J. Theor. Biol. 517 (2021), 110618. https://doi.org/10.1016/j.jtbi.2021.110618.

[21] X.Y. Meng, J. Li, Dynamical behavior of a delayed prey-predator-scavenger system with fear effect and linear harvesting, Int. J. Biomath. 14 (2021), 2150024. https://doi.org/10.1142/s1793524521500248.

[22] A. Kane, K. Healy, T. Guillerme, et al. A recipe for scavenging in vertebrates – the natural history of a behaviour, Ecography 40 (2016), 324–334. https://doi.org/10.1111/ecog.02817.

[23] R.P. Gupta, D.K. Yadav, Complex dynamical behavior of a three species prey–predator system with nonlinear harvesting, Int. J. Bifurcation Chaos 30 (2020), 2050195. https://doi.org/10.1142/s0218127420501953.

[24] P. Panja, Prey-predator-scavenger model with Monod-Haldane type functional response, Rend. Circ. Mat. Palermo, II. Ser 69 (2019), 1205–1219. https://doi.org/10.1007/s12215-019-00462-9.

[25] T.K. Ang, H.M. Safuan, Dynamical behaviors and optimal harvesting of an intraguild prey-predator fishery model with Michaelis-Menten type predator harvesting, Biosystems 202 (2021), 104357. https://doi.org/10.1016/j.biosystems.2021.104357.

[26] M.A. Ahmed, D.K. Bahlool, The influence of fear on the dynamics of a prey-predator-scavenger model with quadratic harvesting, Commun. Math. Biol. Neurosci. 2022 (2022), 62. https://doi.org/10.28919/cmbn/7506.

[27] R.P. Gupta, D.K. Yadav, Role of Allee effect and harvesting of a food-web system in the presence of scavengers, J. Biol. Syst. 30 (2022), 149-181. https://doi.org/10.1142/S021833902250005X.

[28] U. Yadav, S. Gakkhar, Effort dynamics with selective predator harvesting of a ratio-dependent predator-prey system, preprint, (2022). https://doi.org/10.48550/arXiv.2203.11986.

[29] Y.A. Kuznetsov, Tutorial II: One-parameter bifurcation analysis of equilibria with Matcont, Department of Mathematics, Utrecht University, 2011.

[30] R.P. Gupta, P. Chandra, Dynamical properties of a prey-predator-scavenger model with quadratic harvesting, Commun. Nonlinear Sci. Numer. Simul. 49 (2017), 202–214. https://doi.org/10.1016/j.cnsns.2017.01.026.

[31] A.M. Ismael, H.A. Satar, The impact of fear and prey refuge on the dynamics of the food web involving scavenger, Iraqi J. Sci. 64 (2023), 1902-1924. https://doi.org/10.24996/ijs.2023.64.4.29.

[32] R.M. Yaseen, A.A. Mohsen, H.F. Al-Husseiny, et al. Stability and Hopf bifurcation of an epidemiological model with effect of delay the awareness programs and vaccination: analysis and simulation, Commun. Math. Biol. Neurosci. 2023 (2023), 32. https://doi.org/10.28919/cmbn/7910.

[33] Y. Kuang (Ed.), Delay differential equations: with applications in population dynamics, Academic Press, 1993.

[34] Maplesoft, Maplesoft v. 16, Maplesoft, Waterloo, Ontario, Canada, 2008.

[35] B. Ermentrout, XPPAUT 6:00, 2010.

[36] MathWorks, MATLAB v. R2021a, The MathWorks, USA, 2021.

[37] S. Savoca, G. Grifó, G. Panarello, et al. Modelling prey-predator interactions in Messina beachrock pools, Ecol. Model. 434 (2020), 109206. https://doi.org/10.1016/j.ecolmodel.2020.109206.

[38] L. Perko, Differential equations and dynamical systems, Springer, New York, NY, 2001. https://doi.org/10.1007/978-1-4613-0003-8.

[39] H.A. Satar, R.K. Naji, Stability and bifurcation of a prey-predator-scavenger model in the existence of toxicant and harvesting, Int. J. Math. Math. Sci. 2019 (2019), 1573516. https://doi.org/10.1155/2019/1573516.

[40] H.A. Satar, R.K. Naji, Stability and bifurcation in a prey–predator–scavenger system with Michaelis-Menten type of harvesting function, Differ. Equ. Dyn. Syst. 30 (2022), 933–956. https://doi.org/10.1007/s12591-018-00449-5.

[41] W.N.W. Hussin, R. Embong, C.N. Noor, The stability of the critical points of the generalized Gause type predator-prey fishery models with proportional harvesting and time delay, Malays. J. Comput. 6 (2021), 885-897. https://doi.org/10.24191/mjoc.v6i2.9905.